Purification and Characterization of Single-Wall Carbon Nanotubes (SWNTs) Obtained from the Gas-Phase Decomposition of CO (HiPco Process)

I. W. Chiang, B. E. Brinson, A. Y. Huang, P. A. Willis, M. J. Bronikowski, J. L. Margrave, R. E. Smalley, and R. H. Hauge*

Center for Nanoscale Science and Technology, Rice Quantum Institute, Department of Chemistry, MS-60, Rice University, 6100 Main Street, Houston, Texas 77005

Received: April 19, 2001; In Final Form: June 18, 2001

A purification method is given for extracting the Fe metal catalyst and non-SWNT carbon from nanotubes produced by the HiPco process.[1,2] A multistage purification method has been investigated. Sample purity is documented by ESEM, TEM, TGA, Raman and UV-vis−near-IR spectroscopy. Metal catalyzed oxidation at low temperature has been shown to selectively remove non-SWNT carbon and permit extraction of iron with concentrated HCl. Prolonged catalyzed oxidation has been found to preferentially remove smaller diameter tubes. The onset of oxidation of purified smaller diameter HiPco SWNTs is also found to be approximately 100 °C lower than for purified larger diameter tubes produced in the laser-oven process.

Introduction

A high pressure CO disproportionation (HiPco) process, has been shown recently to produce nanotubes of high purity, with current purities of > 90% atomic percent SWNT carbon.[1] In this process, $Fe(CO)_5$ is injected into a stream of CO gas at high temperature and pressure. The iron forms metal clusters that act as catalytic sites to promote the Boudard reaction: $CO + CO \rightarrow C(s) + CO_2(g)$. We believe that when the metal clusters achieve a size near that of C_{60} that they nucleate and grow SWNTs. This occurs because a SWNT is a more stable form of carbon than a near spherical carbon overcoat of a metal cluster when diameters are near 1 nm. The SWNT will continue to grow until the metal cluster, which is also growing with addition of residual free iron atoms, reaches a size that favors formation of a carbon shell around the cluster. This ends the growth of the SWNT.

The average diameter of HiPco SWNTs is approximately 1.1 nm, which is typically smaller than SWNTs produced by the laser-oven process, where the average diameter is about 1.3 nm[3]. The dominant impurity in HiPco nanotubes is the metal catalyst, which is encased in thin carbon shells and distributed throughout the sample as 3−5 nm size particles. Four to five atomic percent of Fe is typical in current raw HiPco materials. Our objective in this study is to remove the iron catalyst and its carbon shell as well as other forms of non-SWNT carbon with minimal loss of SWNTs. The approach utilizes the catalytic activity of the 3−5 nm iron particles, which allows the initial selective oxidation of carbon shells because of their proximity to the metal. The exposed metal particles subsequently catalyze the oxidation of other forms of carbon and SWNTs once the carbon shell is removed.

A stepwise procedure is used to minimize the loss of SWNTs. The purification procedures[4−11] are similar to those discussed in the previous purification study of laser-oven-grown tubes.[12] As suggested in the previous paper, metal catalysts from the production of SWNTs accelerate the oxidation rate of carbon at low temperatures. We have found that the metal particles can be exposed with a low temperature, wet Ar/O_2 (or wet air) oxidation step. This appears to breach the carbon shell and convert the metal particles to an oxide and/or hydroxide. The expansion (densities for Fe and Fe_2O_3 are respectively 7.86 and 5.18 g/cm^3) of the metal particle, due to the lower density of the oxide, breaks the carbon shells open and exposes the metal. This is evidenced by the ability of HCl to extract iron only after the wet Ar/O_2 (or wet air) oxidation. In this paper we present purification procedures for HiPco SWNTs and characterization of HiPco SWNTs. Sample purity is documented with TGA, SEM, and TEM. Raman and UV-vis−near-IR spectra are also reported.

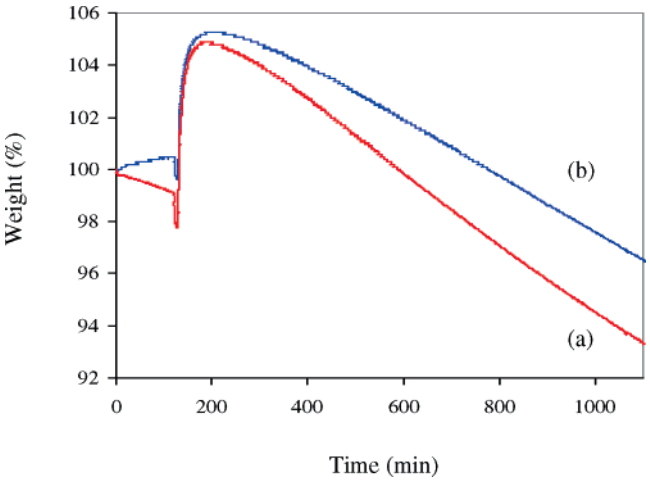

Figure 1. TGA plot of raw HiPco tubes heated at 225 °C for 18 hours in (a) wet Ar/O2, (b) in dry ar/O_2.

Experimental Section

Raw HiPco tubes were subjected to oxidation in a wet Ar/O_2 environment at various temperatures. The addition of water was found to enhanced the low-temperature catalytic oxidation of carbon as shown by TGA in Figure 1. The initial weight gain is due to formation of metal oxide, and the subsequent

* To whom correspondence should be addressed. E-mail: hauge@rice.edu.

10.1021/jp0114891 CCC: $20.00
Published on Web 08/10/2001

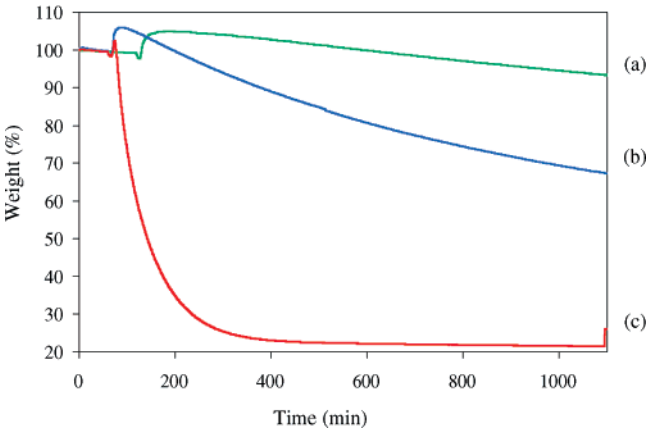

Figure 2. TGA of raw HiPco tubes heated at various temperatures in wet Ar/O_2 for 18, hours* (a) 225 °C, (b) 250 °C, (c) 325 °C. Gas mixture = 20% O_2 in Ar flowing through water bubbler before entering the furnace.

weight loss is due to the removal of carbon. As a result, we have added water to all low-temperature oxidation steps by passing Ar/O_2 (or air) through a room-temperature bubbler. Figure 2 shows the sample weight behavior in wet Ar/O_2 as function of time at different temperatures. Weight gain was observed during the early period of heating for each temperature due to the oxidation of the iron metal particles. The subsequent catalyzed weight loss of carbon is clearly very temperature dependent. No weight loss is observed for low temperature oxidation (e.g., 150 °C or below) after 20 h of heating. When weight loss does occur, it is believed to be due to the loss of carbon shells that are in direct contact with the metal. At temperatures of 225 °C and higher, carbon shells that encase the metal catalysts are removed with an extended oxidation period. Sonication or extended stirring in concentrated HCl solution after oxidation subsequently removes the iron oxides from the processed samples.

All purified HiPco SWNTs in this study were processed as follows: low-density raw HiPco tubes were physically compressed onto a dry filter paper by adding SWNTs to a filter holder while pulling a vacuum. The vacuum helps confine these lightweight samples to the filter holder. This facilitates handling of the raw material whose density is of the order of 0.01 g/cc. SWNTs (typically ~100 mg) were placed in a ceramic boat and inserted into a quartz tube furnace. A gas mixture of 20% O_2 in Ar (air may also be used) was passed through a water bubbler and over the sample at total flow rate of 100 sccm. Nanotubes were heated at 225 °C for 18 h followed by sonication for ~15 min or prolonged stirring (overnight) in concentrated HCl solution. The color of the solution is typically yellow due to dissolved Fe^{3+}. HiPco tubes in the acid solution were then filtered onto a 47 mm, 1.0 μm pore size Teflon membrane (Cole-Parmer) and washed several times with deionized water and methanol. They were dried in a vacuum oven at 100 °C for a minimum of 2 h and weighed. The oxidation and acid extraction cycle was repeated at 325 °C for 1.5 h and 425 °C for 1 h. After drying in the vacuum oven, the HiPco tubes were annealed at 800 °C in Ar for 1 h.

Thermogravimetric (TGA) data was obtained with a TA instrument model 2960 system. Raman spectra were obtained with a Renishaw micro-Raman spectrometer operating with a 780 nm laser. UV-vis−near-IR spectra were obtained with a Shimadzu UV-3101 PC spectrometer. Data from transmission electron microscopy (JEOL 2010 TEM) was obtained using 100 kV beam energy. Raman, IR, and TGA were carried out with

TABLE 1: Weight Loss and Metal Concentration after Each Purification Step[a]

sample	metal %[b]	weight loss[c]
(a) raw HiPco	5.06	
(b) raw HiPco tubes heated at 225 °C in wet Ar/O_2 for 18 h	0.67	33.7%
(a) heated at 325 °C in wet Ar/O_2 for 1.5 h	0.05	8.3%
(b) heated at 425 °C in wet Ar/O_2 for 1 h	0.03	22.9%
(d) annealed in Ar at 800 °C for 1 h	0.03	4.2%

[a] Each oxidation step is followed by sonication in concentrated HCl solution for 10−15 min. Tubes were then filtered and dried from the acid solution in a vacuum oven at 100 °C for a minimum of 2 h. [b] Metal % = Fe percent, which is calculated as Fe atomic perecent/(C+Fe) atomic percent from the TGA data. [c] Total weight loss = 69.1%; total weight loss excluding the 425 °C step = 46.25%.

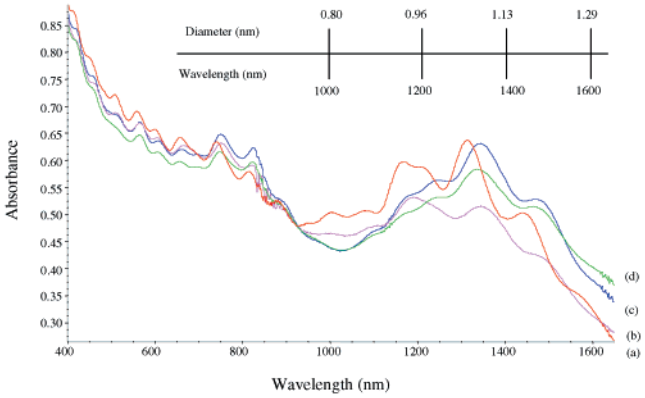

Figure 3. UV-vis−near-IR spectra of HiPco SWNTs: (a) raw HiPco tubes, (b) after 225 °C oxidation step, (c) and (b) after 325 °C oxidation step*, (d) and (c) after 425 °C oxidation step. Each oxidation step is completed by HCl sonication, vacuum-drying and, annealing at 800 °C in Ar for 1 hour. Spectra have been normalized at 925 nm and scale bar shows adjusted tube diameter.[4]

SWNTs in the form of solids. Samples for UV-vis−near-IR were prepared by sonicating SWNTs for ~10 min in 1,2-dichlorobenzene solution in a bath sonicator (Cole-Parmer). TEM samples were prepared by sonicating SWNTs in methanol and drop drying onto lacey carbon TEM grids.

It is useful to weigh the sample before and after each cleaning step as a measure of how much metal and carbon have been removed. A typical weight loss and metal concentration after each purification step is shown in Table 1. The Fe atomic percentage drops from ~3.5% to 0.02%, as obtained from residual Fe_2O_3 weights in TGA measurements. The weight loss is seen to increase dramatically from the 325 °C to the 425 °C step. UV-vis−near-IR spectra indicate a preferential loss of smaller diameter tubes during the cleaning process (Figure 3). SEM images (Figure 4) of raw and cleaned samples suggest some rearrangement of SWNTs into slightly larger ropes. TGA data for purified HiPco SWNTs illustrate that the SWNTs are able to withstand oxidation temperatures as high as 500 °C (Figure 5). With each cleaning step less metal remains and the onset oxidation temperature is seen to increase. The small change between the 325 °C and 425 °C oxidation steps suggests that oxidation above 325 °C provides little additional air stability, most likely because little iron remains after the 325 °C step. TEM images after cleaning show a large reduction of metal and non-SWNT carbon (Figure 6). The dispersibility of cleaned HiPco tubes before high temperature annealing is observed to be just as good as the raw HiPco SWNTs. We find

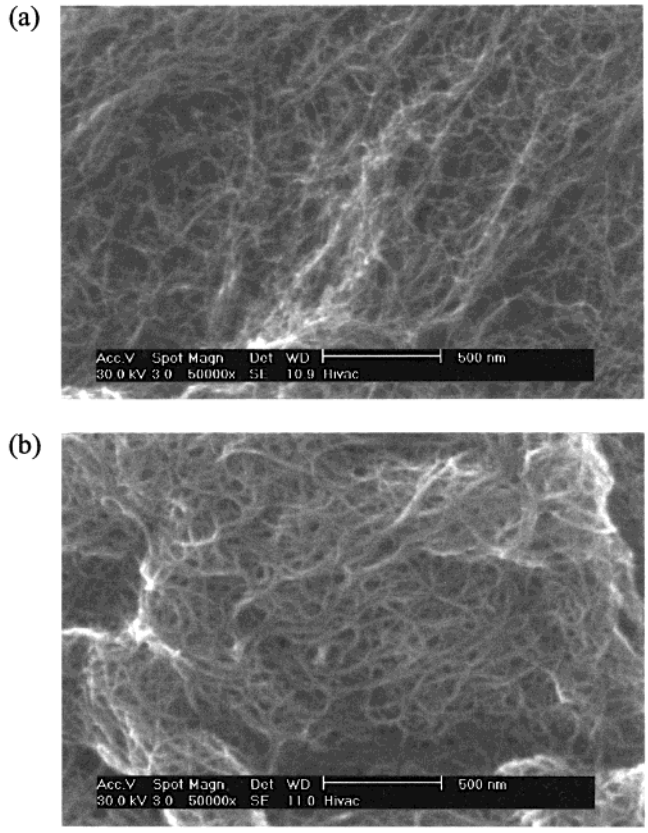

Figure 4. SEM images of HiPco tubes: (a) raw HiPco SWNTs, (b) purified SWNTs.

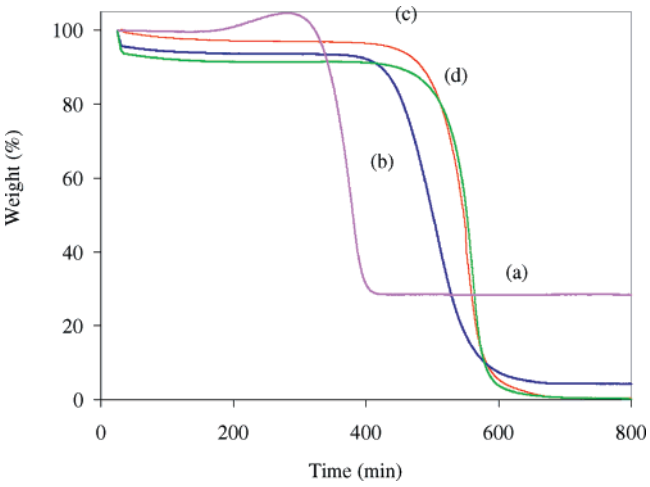

Figure 5. TGA of Purified HiPco SWNTs: (a) raw HiPco, (b) after 225 °C step, (c) after 325 °C step, (d) after 425 °C step. Each step is completed after HCl extraction of metals and vacuum-drying. All samples were subsquently annealed at 800 °C in Ar for 1 hour.

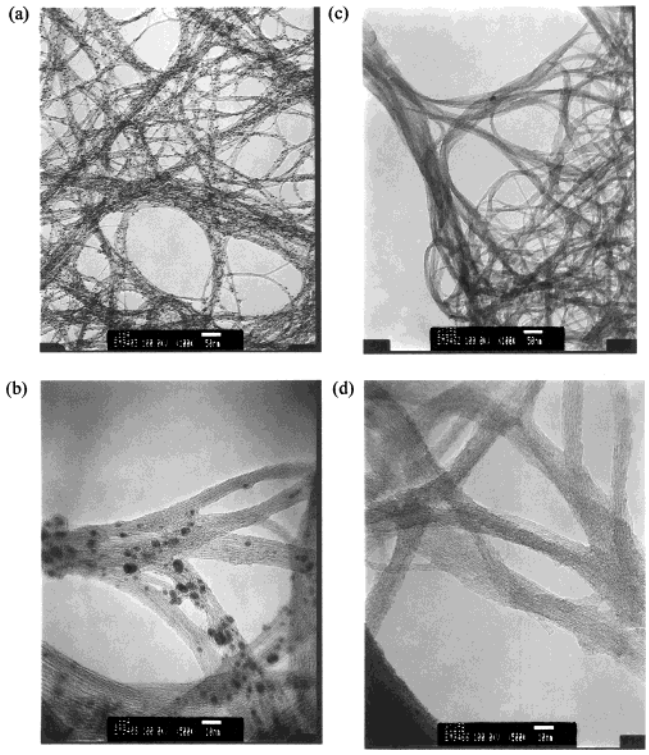

Figure 6. TEM images of HiPco SWNTs. Raw HiPco tubes: (a) magnification 100 K, (b) magnification 500 K. Purified HiPco tubes: (c) magnification 100 K, (d) magnification 500 K.

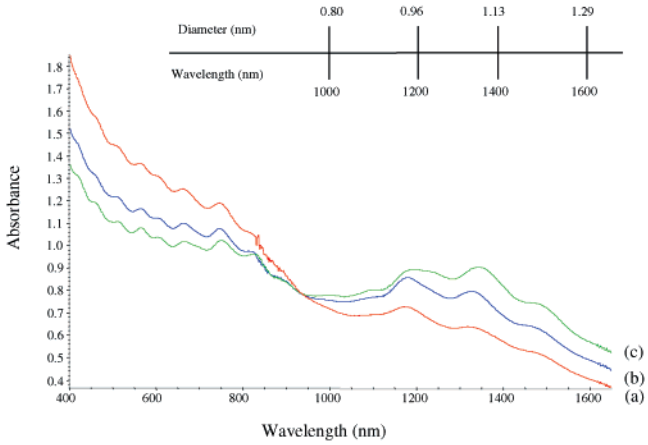

Figure 7. UV-vis−near-IR spectra of purified HiPco SWNTs: (a) raw HiPco SWNTs after 225 °C oxidation, HCl sonication, and vacuum-drying, (b) sample of (a) neutralized with 2 M NaOH solution, (c) sample of (a) annealed at 800 °C in Ar. Spectra have been normalized at 925 nm and scale bar shows adjusted tube diameter.

that the clean samples are more difficult to disperse after high temperature annealing presumably because larger more well-ordered rope structures are formed at high temperatures.

Spectra for neutralization effects are shown in Figure 7. We have consistently found that if SWNTs have experienced an acidic environment that the relative intensities of the long wavelength van Hove features are reduced relative to shorter wavelength features. However, if the sample is subsequently exposed to a basic solution, the relative intensities of the long wavelength features increase as shown in Figure 7. We attribute this effect to protonation of SWNTs during acid exposure, where the most energetically available electrons (those responsible for the long wavelength van Hove features) interact most strongly with the adsorbed protons. During exposure to acids it is likely that some of the acid intercalates into SWNT ropes such that simple vacuum-drying at low temperatures does not remove all of the acid. Subsequent exposure to a basic solution with stirring or sonication does remove this residual acid and restores the intensity of the van Hove features. A similar increase in the relative intensities of the van Hove features occurs when cleaned samples are annealed in Ar at 800 °C. In this case, the small amounts of residual acid are removed due to effective desorption at the high temperatures.

The relative intensities of Raman spectra after each step appear to mirror the changes observed in electronic spectra. This is shown in Figure 8 where a loss of intensity is observed for

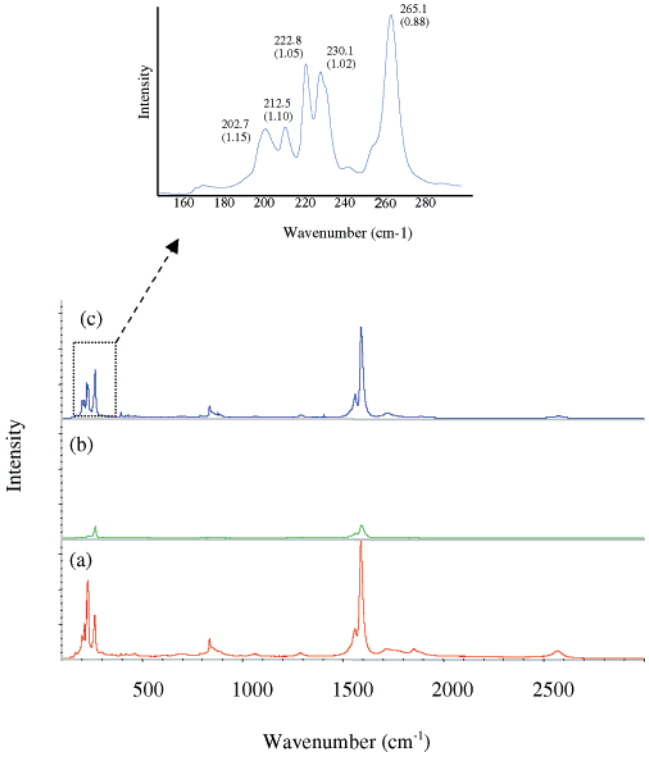

Figure 8. Raman spectra of purified HiPco SWNTs: (a) raw HiPco SWNTs, (b) sample of (a) after 225 °C oxidation, HCl sonication, and vacuum-drying, (c) sample of (b) after annealing at 800 °C in Ar.

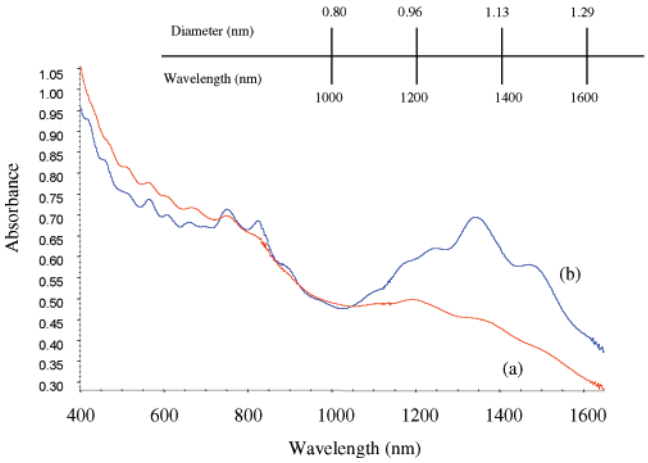

Figure 9. UV-vis−near-IR spectra of purified HiPco SWNTs annealed at 800 °C in Ar (a) in wet Ar, (b) in dry Ar. Spectra have been normalized at 925 nm and scale bar shows adjusted tube diameter.

the cleaned but not annealed sample. We also note a change in relative intensity for various peaks in the low frequency breathing mode from the raw sample to the annealed clean sample, which suggests that the content of smaller diameter SWNTs has increased relative to the larger diameter ones. However, it is likely that this intensity change is due to a different coupling of the electronic resonance enhanced spectra to the Raman laser (782 nm) rather than to a relative change in tube diameter populations in the cleaned sample. In fact, electronic spectra, which we believe to be a more reliable measure of tube diameter distribution, previously shown in Figure 3, indicate that small diameter tubes are preferentially lost in the cleaning process.

An interesting dependence of the electronic spectra of cleaned SWNTs on annealing conditions, wet or dry in Ar at 800 °C, was observed (Figure 9). Dry annealing gives spectra with a

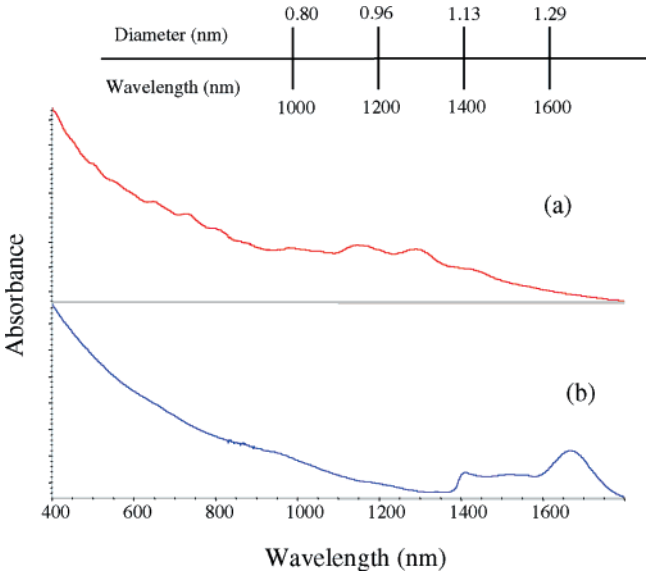

Figure 10. UV-vis−near-IR spectra of HiPco vs laser-oven-grown SWNTs: (a) HiPco SWNTs, (b) laser-oven-grown SWNTs.

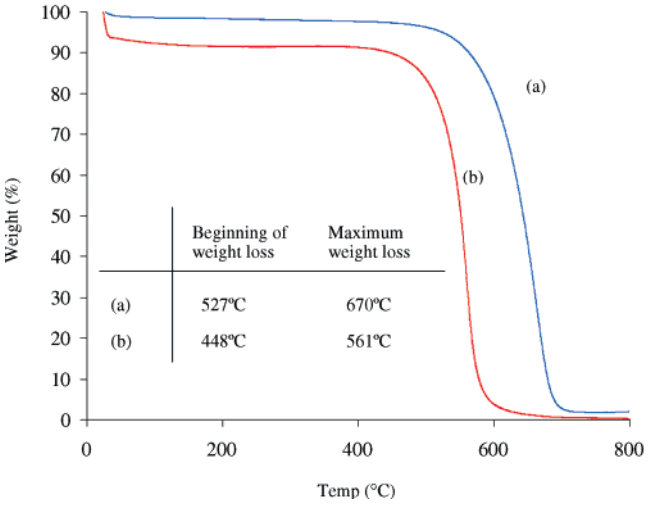

Figure 11. TGA plots of HiPco vs laser-oven-grown SWNTs: (a) laser-oven-grown SWNTs, (b) HiPco SWNTs. Samples were heated in air to 800 °C at 5 °C/min.

greater intensity of the long wavelength van Hove features. We have also found that clean HiPco tubes annealed in wet Ar have more difficulty dispersing into 1,2-dichlorobenzene solution than do dry Ar annealed tubes. The same wet Ar annealed sample, however, is observed to disperse better in 0.15 wt. % Triton-X water solution than the dry annealed. A loss of intensity in the long wavelength van Hove features has been previously observed when SWNTs are sidewall functionalized.[13] This suggests that wet annealing in Ar at 800 °C leaves the SWNTs partially functionalized with hydroxyl groups.

Discussion

It is interesting at this point to compare SWNTs that have been produced by different methods. In this case we compare SWNTs that have been produced by the laser-oven process to tubes produced by the high pressure CO (HiPco) process. It is clear that diameter size distributions differ considerably when one compares the UV-vis−near-IR spectra as shown in Figure 10 for SWNTs produced by the two processes. Clearly the HiPco process produces a smaller diameter size distribution. TGA studies of the air stability of cleaned SWNTs from the two

processes, as shown in Figure 11, indicate that laser oven SWNTs are more stable in air than are HiPco SWNTs. Since the metal has been removed from both samples, we believe this reflects a higher reactivity with oxygen for small diameter tubes than for large diameter tubes. This appears to be consistent with the greater steric strain present in small diameter SWNTs.

Acknowledgment. This work was supported by Robert A. Welch Foundation, the Advanced Technology Program of Texas, the National Aeronautics and Space Administration, Office of Naval Research, and the National Science Foundation.

References and Notes

(1) Nikolaev, P.; Bronikowski, M. J.; Bradley, R. K.; Rohmund, F.; Colbert, D. T.; Smith, K. A.; Smalley, R. E. *Chem. Phys. Lett.* **1999**, *313*, 91.

(2) Bronikowski, M. J.; Willis, P. A.; Colbert, D. T.; Smith, K. A.; Smalley, R. E. *J. Vac. Sci. Technol., A* **2001**, *19*(4), 1800.

(3) Thess, A.; Lee, R.; Nikolaev, P.; Dai, H. J.; Petit, P.; Robert, J.; Xu, C. H.; Lee, Y. H.; Kim, S. G.; Rinzler, A. G.; Colbert, D. T.; Scuseria, G. E.; Tománek, D.; Fischer, J. E.; Smalley, R. E. *Science* **1996**, *273*.

(4) Hidefumi, H. *Mol. Cryst. Liq. Cryst. Sci. Technol., Sect. A* **1995**, 276, 267.

(5) Yumura, M.; Uchida, K.; Niino, H.; Ohshima, S.; Kuriki, Y.; Yase, K.; Ikazaki, F. *Mater. Res. Soc. Symp. Proc. Novel Forms of Carbon II* **1994**, 349, 231.

(6) Dillon, A.; Gennett, T.; Jones, K.; Alleman, J.; Parilla, P.; Heban, M. *Adv. Mater.* **1999**, 16, 1354.

(7) Bandow, S.; Zhao, Z.; Ando, Y. *Appl. Phys.* A **1999**, 67, 23.

(8) Rinzler, A.; Liu, J.; Dai, H.; Nikolaev, P.; Huffman, C.; Rodriguez-Macias, F.; Boul, P.; Lu, A.; Heymann, D.; Colbert, D. T.; Lee, R.; Fischer, J.; Rao, A.; Eklund, P.; Smalley, R. E. *Appl. Phys. A* **1998**, 67, 29.

(9) Dujardin, E.; Ebbesen, T.; Krishnan, A.; Treacy, M. *Adv. Mater*. **1998**, 10, 611.

(10) Hiura, H.; Ebbesen, T.; Tanigaki, T. *Adv. Mater*. **1995**, 7, 275.

(11) Zimmerman, J.; Bradley, R.; Huffman, C.; Hauge, R. H.; Margrave, J. L. *Chem. Mater*. **2000**, 12, 1361.

(12) Chiang, I. W.; Brinson, B. E.; Smalley, R. E.; Margrave, J. L.; Hauge, R. H. *J. Phys. Chem. B* **2001**, *105*, 1157.

(13) Boul, P. J.; Liu, J.; Mickelson, E. T.; Huffman, C. B.; Ericson, L. M.; Chiang, I. W.; Smith, K. A.; Colbert, D. T.; Hauge, R. H.; Margrave, J. L.; Smalley, R. E. *Chem. Phys. Lett* **1999**, *310*, 367.